Journal of Hydrology: Regional Studies 4 (2015) 516–534

Contents lists available at ScienceDirect

Journal of Hydrology: Regional Studies

journal homepage: www.elsevier.com/locate/ejrh

Sediment yields from small, steep coastal watersheds of California

Jonathan A. Warrick[a,*], John M. Melack[b], Blair M. Goodridge[b,c]

[a] U.S. Geological Survey, 400 Natural Bridges Rd, Santa Cruz, CA, USA
[b] Bren School of Environmental Science and Management, University of California, Santa Barbara, CA, USA
[c] Marine Science Institute, University of California, Santa Barbara, CA, USA

ARTICLE INFO

Article history:
Received 5 May 2015
Received in revised form 4 August 2015
Accepted 19 August 2015

Keywords:
Suspended-sediment discharge
Sediment yield
Coastal California mountains
Watersheds

ABSTRACT

Study region: Coastal watersheds of southern California, United States.
Study focus: We sought to better understand the rates and variability of suspended-sediment discharge from small coastal watersheds (<100 km^2) of California. Suspended-sediment concentrations and stream discharge were measured with automated samplers near the mouths of four small watersheds (10–56 km^2).
New hydrological insights for the region: The watersheds were found to have suspended-sediment concentrations that extended over five orders of magnitude (1 to over 100,000 mg L^{-1}). Sediment concentrations were weakly correlated with discharge (r^2 = 0.10–0.25), and four types of hysteresis patterns were observed during high flow events (clockwise, counterclockwise, no hysteresis, and complex). Annual sediment yields varied by 400-fold across the four watersheds (e.g., 5–2100 t km^{-2} yr $^{-1}$ during the 2003–2006 water years), and sediment discharge was measurably elevated in one watershed that was partially burned by a late summer wildfire. Dozens of high flow events provided evidence that suspended-sediment yields were generally related to peak stream discharge and event-based precipitation, although these relationships were not consistent across the watersheds. This suggests that watersheds smaller than 100 km^2 can provide large – and therefore important – fluxes of sediment to the coast, but that simple techniques to estimate sediment loads, such as sediment rating curves, hydrologic regressions, and extrapolation using global sediment yield relationships that include watershed area as a primary factor, may provide poor results.

1. Introduction

Small, steep watersheds along land–ocean margins discharge ecologically and geologically relevant masses of sediment, nutrients, carbon and other constituents into the world's oceans (Milliman and Syvitski, 1992; Lyons et al., 2002; Beusen et al., 2005; Milliman and Farnsworth, 2011). Although it has been estimated that over half of the sediment discharged to the sea originates from the cumulative discharge of watersheds smaller than 10,000 km^2 (Milliman and Syvitski, 1992), these computations are hindered by a scarcity of data from the smallest coastal watersheds. For example, the most thorough global database to date by Milliman and Farnsworth (2011) effectively captures ~82% of the ~105 million km^2 of land area

* Corresponding author.
E-mail address: jwarrick@usgs.gov (J.A. Warrick).

http://dx.doi.org/10.1016/j.ejrh.2015.08.004
2214-5818/

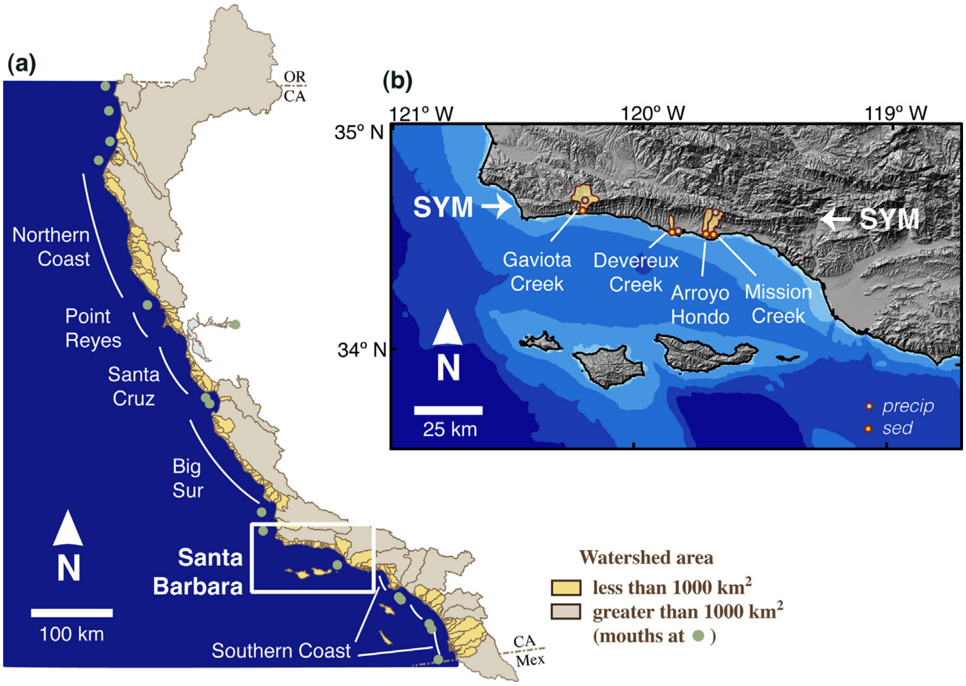

Fig. 1. Coastal watersheds of California and the Santa Barbara study area. (a) Watersheds of the California coast, highlighting the smallest of these watersheds (i.e., those with drainage areas less than 1000 km^2) in yellow. Coastal regions receiving drainage primarily from these smaller watersheds are named and labeled. (b) The Santa Barbara Channel coastal region including four watersheds draining the Santa Ynez Mountains (SYM) that were monitored for this study. (For interpretation of the references to colour in this figure legend, the reader is referred to the web version of this article.)

draining to the world's oceans. Although this database includes hundreds of watersheds smaller than 10,000 km^2, there are over ten thousand coastal watersheds ranging between 10 and 10,000 km^2 – and representing roughly 18% of the Earth's land surface – for which no discharge data exist (Milliman and Farnsworth, 2011).

Thus, global biogeochemical inventories lack information from the smallest watersheds of the world, which likely have high yields of sediment, nutrients and carbon (Vörösmarty et al., 2000; Gomez et al., 2003; Ludwig et al., 2009; Milliman and Farnsworth, 2011). It is, therefore, important to better quantify material fluxes from small coastal watersheds to better constrain regional and global assessments of biogeochemical cycles including sediment budgets.

At regional scales, such as the coast of California in North America (Fig. 1a), small watersheds are the only drainage type for long coastal stretches. For example, the 'Northern Coast' and the 'Big Sur' coastal regions of California are both over 150 km long yet have no watersheds greater than 1000 km^2 draining into them (Fig. 1a). Although there is a scarcity of discharge information for these smaller watersheds (cf. Farnsworth and Warrick, 2007), there is substantial need for these data largely owing to the high marine biodiversity and productivity along these steep, rugged coastal sections (Duggins et al., 1989; Croll et al., 2005) and the potential for fluvial inputs to these marine systems to influence habitats, water quality and ecosystem functions (Warrick et al., 2005; Page et al., 2008; Foley and Koch, 2010; Goodridge and Melack, 2012).

Substantial improvements have occurred in the hydrologic monitoring techniques and understanding of small mountainous watersheds, although much of this understanding has arisen from the study of headwater tributaries within larger watersheds (de Vente et al., 2011; Hinderer et al., 2013). These headwater studies suggest that there are fundamental differences in the frequency and magnitude of sediment discharge in the smaller, low-order drainage basins compared to the larger, high-order drainage basins (Walling, 1974; Graft, 1988). For example, sediment discharge from small watersheds is commonly ephemeral, and the majority of the long-term sediment discharge occurs during and immediately following infrequent heavy precipitation when suspended-sediment concentrations can rise to grams or hundreds of grams per liter (Tropeano, 1991; Coppus and Imeson, 2002; Milliman and Kao, 2005; Galewsky et al., 2006; Mano et al., 2009; Grodek et al., 2012; Conaway et al., 2013). Additionally, several factors can exacerbate erosion within and sediment yields from these small watersheds, including: ground shaking from seismic activity (Dadson et al., 2004; Hovius et al., 2011); vegetation clearing and sediment release after wildfire (Shakesby and Doerr, 2006; Malmon et al., 2007; Lamb et al., 2011; Warrick et al., 2012), glacial processes (Hinderer et al., 2013); shifts in climate (Galewsky et al., 2006); geomorphic change of the watershed landscape (Nearing et al., 2007; Nadal-Romero and Regüés, 2010); human-derived disturbances from land use and channel alterations (Trimble, 1981, 1997; Owens et al., 2010; de Vente et al., 2011); and combinations of these effects (Madej and Ozaki, 1996; Pinter and Vestal, 2005; Warrick and Rubin, 2007; García-Ruiz et al., 2013).

The coastal watersheds of the Santa Barbara Channel region (Fig. 1) provide an excellent setting to sample and characterize sediment discharge from small watersheds, owing to the long, straight Santa Ynez Mountain range that results in a series of southward draining watersheds with relatively similar basin characteristics and easily accessible sampling locations near the mouths of these drainages (Duvall et al., 2004; Warrick and Mertes, 2009). The region has also been the focus of previous studies of hydrology, sediment yield and marine ecology (e.g., Keller et al., 1997; Gabet and Dunne, 2002; Warrick and Mertes, 2009; Washburn and McPhee-Shaw, 2013; Brzezinski et al., 2013), which allows for comparisons and potential extrapolations as noted below. Here we provide analysis of new sediment discharge data from a series of Santa Ynez Mountain watersheds to address the following research questions: (i) How and why do sediment yields vary in time and space? (ii) Can the measured sediment yields be extrapolated across the study area?

To address these research questions we collected and evaluated measurements of suspended-sediment concentration and discharge from four small watersheds (10–52 km^2) of the Santa Ynez Mountains of California (Fig. 1). These watersheds are located in the high sediment yield region of the Western Transverse Ranges (Brownlie and Taylor, 1981; Willis and Griggs, 2003; Warrick and Mertes, 2009). Previous analyses of sediment discharge from Santa Ynez Mountain watersheds by Warrick and Mertes (2009) revealed that spatial and temporal variability existed in stream suspended-sediment concentrations. Additionally, Keller et al. (1997) and Coombs and Melack (2012) showed that wildfire in the Santa Ynez Mountains dramatically increased post-fire sediment yields. Our study adds to these previous studies by providing new observations of the timing and rates of sediment discharge from intensive sampling from four small, steep watersheds of the Santa Ynez Mountains. These observations add several additional years of data from a watershed (Gaviota Creek) evaluated by Coombs and Melack (2012), and include several watersheds (Devereux Creek, Arroyo Burro and Mission Creek) that have never been sampled intensively.

2. Study area

The Santa Ynez Mountains are an east-west trending range within the broader Western Transverse Ranges of California, and these mountains define the northern land-boundary of the Santa Barbara Channel (Fig. 1). Transpression of the Western Transverse Ranges since the Pliocene (ca. 3 Ma) has resulted in the uplift of the Santa Ynez Mountains, which are dominantly marine siltstones, sandstones and shales (Luyendyk, 1991). Tectonic uplift of the Santa Ynez Mountains has continued through modern times at average rates of 0.8–5 $mm\,yr^{-1}$ as shown by marine terraces and stream profiles (Duvall et al., 2004). These rates of tectonic uplift and mountain building within the broader Western Transverse Ranges result in landscape erosion and sediment export to the sea at rates that are several times to orders of magnitude higher than other mountain ranges of California (Brownlie and Taylor, 1981; Inman and Jenkins, 1999).

Seventy-four small watersheds, with a total area of 790 km^2, drain from the Santa Ynez Mountains from the mountain crest (max. elevation = 1482 m) to the coast of the Santa Barbara Channel (Fig. 1b). Several of the smallest watersheds of the region, such as Devereux Creek (9.6 km^2; Fig. 1b), drain only a portion of the lower Santa Ynez Mountains (Duvall et al., 2004). The largest watershed of the region is Gaviota Creek (52 km^2; Fig. 1b), which is the only basin that drains both the southern and north aspects of the Santa Ynez Mountains and is likely a relic drainage that persisted through the orogeny of the mountain range.

Water and sediment discharge in the Santa Ynez Mountain watersheds are ephemeral, highest following winter precipitation and often negligible during the dry summers (Beighley et al., 2003; Warrick and Mertes, 2009). Precipitation is generated by frontal storms from the northern Pacific, and orographic enhancement results in an increase in precipitation between the coast (~50 $cm\,yr^{-1}$) and the mountain crest (~85 $cm\,yr^{-1}$). Annual precipitation is highly variable, and precipitation during wet years can be 2-3 times long-term averages (Beighley et al., 2003). Stream discharge of water is punctuated and flashy during the wet winter season, with most of the annual flow occurring in only a few days per year (Beighley et al., 2003).

Erosional processes in the Western Transverse Ranges include, in approximate decreasing order of importance for sediment production: mass movements, dry ravel, stream-bank erosion, and sheet flow (Rice and Foggin, 1971; Taylor, 1981; Rice, 1982; Hill and McConaughy, 1988; Raphael et al., 1995; Lavé and Burbank, 2004). The conversion of native chaparral to non-native grasses has been widespread in the lowlands of many of the watersheds, and these land cover changes have increased soil erosion and landslide frequencies in the region (Cole and Liu, 1994; Gabet and Dunne, 2002; Pinter and Vestal, 2005; Ejarque et al., 2015). Wildfires are common in the coastal chaparral that dominates the Santa Ynez Mountain landscape, and the incineration of vegetation from fire can exacerbate sediment production, especially if the subsequent winter has heavy precipitation (Florsheim et al., 1991; Keller et al., 1997; Lamb et al., 2011; Coombs and Melack, 2012). Periodic wildfires are suggested to increase the magnitude of millennial-scale sediment yields in the region by 10 to 100 percent (Wells, 1981; Lavé and Burbank, 2004; Warrick et al., 2012).

A summary of the published sediment yield values for the Santa Ynez Mountain region is provided in Table 1. Average sediment yields are estimated to be 1500–2700 $t\,km^{-2}\,yr^{-1}$, and these rates can increase by an order of magnitude within watersheds burned by wildfire during the first year following a burn. Suspended-sediment concentrations over 150,000 $mg\,L^{-1}$ have been measured in the region's streams following the first precipitation after wildfire (Warrick and Mertes, 2009; Coombs and Melack, 2012). Evidence of these high sediment concentrations are recorded in gravity flow deposits on the continental shelf offshore of the Santa Ynez Mountains formed by plunging, or hyperpycnal, discharge conditions at the watershed mouths initiated by high sediment concentrations (Warrick et al., 2013b).

Table 1
Published sediment yield values from investigations of the Santa Ynez Mountain watersheds.

Sediment yield ($t\,km^{-2}\,yr^{-1}$)	Measurements	Duration of study	Watershed and drainage area (km^2)	Reference
$2350\,t\,km^{-2}\,yr^{-1}$[a,b] (partially burned)	Debris basin and wetland sedimentation after wildfire	2 years (1991–1992)	Goleta Slough creeks ($50.08\,km^2$) (23.7% burned)	Keller et al. (1997)
$1500\,t\,km^{-2}\,yr^{-1}$	Suspended-sediment sampling (extrapolated)[c]	72 years (1928–1999)	7 creeks ($5–40\,km^2$)	Warrick (2002)
$1000\,t\,km^{-2}\,yr^{-1}$[b] (littoral-grade sand and gravel greater than 0.125 mm)	Debris basin sedimentation[d]	44 years (1964–2008)	16 debris basins in 10 watersheds ($104\,km^2$ total captured area)	Warrick (2009)
$2600–3800\,t\,km^{-2}\,yr^{-1}$ (partially burned)	Suspended-sediment sampling after wildfire	1 year (2005)	Gaviota Creek ($52\,km^2$); Arroyo Honda ($11\,km^2$)	Coombs and Melack (2012)
$18,100\,t\,km^{-2}\,yr^{-1}$ (fully burned)	Suspended-sediment sampling after wildfire	1 year (2005)	San Onofre ($5\,km^2$)	Coombs and Melack (2012)
$5-2100\,t\,km^{-2}\,yr^{-1}$	Suspended-sediment sampling	4 years (2003–2006)	This study	This study

[a] $147,000\,m^3$ of sediment deposited over a two year interval of time from the combined Goleta Slough creeks.
[b] Assumes a $1.6\,t\,m^3$ bulk density for sediment.
[c] Suspended-sediment rating curves developed from combining all data from seven watersheds collected over 3 winter seasons and extrapolating the rating curve to 1928–1999.
[d] There is presumed, but uncalculated, bias in these data owing to the construction and subsequent monitoring of debris basins following wildfires.

3. Methods

3.1. Site selection

Four watersheds of the Santa Ynez Mountains were sampled for stream discharge, sediment concentrations and precipitation between 2004 and 2009. These watersheds represent a range of watershed types in the region, including two steep basins draining from the crest of the Santa Ynez Mountains to the coast (Arroyo Burro and Mission Creek), one relatively flat basin that drains only the lowland landscape below the mountain crest (Devereux Creek), and one relatively steep basin that drains through the Santa Ynez Mountains (Gaviota Creek; Fig. 1b; Tables 2 and 3). Although Gaviota Creek data from water year 2005 were evaluated in Coombs and Melack (2012), here we expand upon these analyses by including data from this watershed during two additional water years.

3.2. Sampling and analyses

Stream stage and water sampling were conducted with the use of pressure transducers and pumped auto-samplers at each station as described by Coombs and Melack (2012) and Goodridge and Melack (2012). Stream stage was measured for each station at 5-min intervals using pressure transducers (Solinst Levelogger Model 3001) corrected for local atmospheric pressure. Stage records were converted to discharge estimates using rating relationships developed from the combination of U.S. Army Corps of Engineers' Hydrologic Engineering Center River Analysis System (HEC-RAS) and periodic manual discharge measurements with a current meter. As noted by Coombs and Melack (2012), the uncertainty in the discharge estimates were 5–10% during flows greater than $3\,m^3\,s^{-1}$. Stations were located at the lowest feasible point in the watershed without tidal influence on water stage (Table 3).

Sediment concentrations of the stream waters were measured primarily from samples collected with auto-samplers (ISCO 6712C) with 1-cm diameter intakes and tubing. Inlets for the samplers were anchored above the channel bed and as near to the thalweg as possible. While these techniques are less than ideal compared to standard flow-integrated sampling techniques such as those described by Guy and Norman (1970), they were considered adequate for the study site owing to: (i) the high stream velocities (meters per second) and rapidity of flow dynamics during runoff events which made manual sampling too dangerous for field technicians (cf. Warrick and Mertes, 2009), (ii) the dominance of fine-grained sediment (silt and clay) in the suspended-sediment loads owing to the marine sedimentary parent material, which combined with the high stream velocities, was hypothesized to result in well-mixed profiles of suspended-sediment in these streams (cf. Warrick, 2002; Clark et al., 2009; Warrick et al., 2012), and (iii) the rapidity of variations in flow and suspended-sediment conditions during precipitation events that made it impossible to manually sample these unsteady conditions across several watersheds.

Table 2
Monitoring stations and watershed information for this study.

	Gaviota Creek	Devereux Creek	ArroyoBurro	Mission Creek
Drainage area (km^2):	52.1	9.6	25.4	30.0
Relief (m):	851	168	1195	1208
Mean Slope (deg):	30	5	28	27
Land cover (% area):[a]				
Forest and shrub:	58	3	45	45
Urban:	0	77	43	53
Rangelands:	41	11	5	0
Agriculture:	0	6	7	2
Other:	1	0	0	1
Sediment discharge:				
Station name[b]:	GV01	DV01	AB00	MC00
Latitude:	34.4855°	34.4176°	34.4051°	34.4131°
Longitude:	120.2292°	119.8741°	119.7402°	119.6950°
Water years active:	2003, 2005, 2006	2004–2006	2003–2005	2003–2006
Number of sediment samples:	606	374	473	655
Precipitation:				
Station name[b]:	GV202	UCSB200	El Deseo 255	El Deseo 255
Operator:	UCSB LTER	SB County	SB County	SB County
Latitude:	34.5077°	34.4150°	34.4917°	34.4917°
Longitude:	120.2286°	119.8461°	119.6958°	119.6958°
Water years active:	2003–2006[c]	2003–2006	2003–2006	2003–2006

[a] land cover after remote sensing analyses of Goodridge and Melack (2012); sum of land cover may not equal 100% owing to rounding.
[b] Station names as denoted in the Santa Barbara Channel LTER database (http://sbc.lternet.edu//data/index.html).
[c] Data gap occurred during spring of 2005, which was filled using observations from GV201 (34.4801°, 120.2292°) and the best-fit linear regression between these stations (slope = 0.819, offset = 0, lag = 0.0 h).

Table 3
Comparison of sediment concentration hysteresis patterns for the study area stations.

	Gaviota Cr.	Devereux Cr.	Arroyo Burro	Mission Cr.
Hysteresis of measurable events:				
Clockwise:	3 (11%)	4 (17%)	3 (10%)	6 (14%)
Counterclockwise:	8 (30%)	2 (8%)	9 (29%)	6 (14%)
No hysteresis:	5 (19%)	9 (38%)	7 (23%)	7 (17%)
Complex:	11 (41%)	9 (38%)	12 (39%)	23 (55%)

To test the assumption of well-mixed sediment concentration profiles, thirty-five grab samples of the stream water surface were obtained from four watersheds during storms while the autosamplers were actively sampling. The mean and geometric means of the surface water suspended-sediment concentrations were 8300 and 1700 mg L^{-1}, respectively, and linear regression between the autosampled and surface grab concentrations resulted in a slope of 0.80 ± 0.05 and r^2 of 0.85. The linear relationship between these skewed data sets was tested with a non-linear, power law regression that resulted in a power-law exponent of 1.004 and a constant of proportionality of 0.75 (r^2 = 0.92). Thus, the surface water sediment concentrations were consistently ~80% of the near-bed concentrations. Using theoretical Rouse profiles of suspended-sediment concentrations following the van Rijn (1984) formulations as described in the supplemental information of Warrick et al. (2012) and fitting a representative sediment settling velocity to ensure a 80% ratio of near-surface to near-bed sediment concentrations for flow speeds of 0.5–3 m s^{-1}, it was found that near-bed concentrations would be consistently 15% higher than flow-averaged sediment concentrations over the entire water profile. This slight bias was corrected for in the sediment discharge and yield calculations as noted in Section 3.3 below.

Hence, although suspended-sediment concentrations can vary considerably with depth and distance across a stream channel especially in low gradient settings (Horowitz et al., 1990), we suggest that the steep stream channel settings and vigorous mixing of suspended sediment at our study sites resulted in conditions analogous to alpine streams and urban runoff channels, for which pumped samplers have been shown to provide relatively unbiased measurements of suspended-sediment concentrations (Gurnell et al., 1992; Roseen et al., 2011).

To focus on the intervals of time with the greatest transport of sediment, sampling frequency increased with flow rate. For example, during the low flow conditions of May–October water samples were taken once every other week. Higher sampling frequencies occurred during the remainder of the year, including weekly samples from November to April and samples every 1–4 h during and following precipitation events. Several hundred samples were collected for each station (Table 2).

One of two analysis methods was used to measure suspended-sediment concentrations of the water samples based on a visual estimates of the amount of sediment in each sample bottle. If samples contained less than ~1000 mg L^{-1}, suspended-sediment concentrations were measured by filtering measured volumes of sample onto pre-tared filters (Gelman A/E filter, 47 mm) that were subsequently dried at 105 °C for 2 h and weighed. If samples contained greater than ~1000 mg L^{-1}, suspended-sediment concentrations were calculated with three measured weights of the polypropylene sample bottle: (i) full with the sediment and water mixture, (ii) the bottle and sediment following removal of the water from clear water decanting, heating to remove all visible water, and drying at 105 °C for 2 h, and (iii) the dry, empty bottle. These two methods were consistent with methods A and B outlined by ASTM D 3977-97.

Precipitation measurements were obtained from tipping bucket rain gauges sampled at 5-min increments. These data include a stations operated by our research group and by the Santa Barbara County Flood Control District (Table 2). All data presented here and additional data from other stations in the study area are available from the Santa Barbara Coastal Long Term Ecological Research (SBC LTER) project (http://sbc.lternet.edu/; accessed 22.07.15).

3.3. Computational methods

The discharge and suspended-sediment measurements were used to evaluate the time-dependent relationships of suspended-sediment concentrations, discharge and yield. Owing to the strong relationship between discharge and sediment concentrations for California watersheds (e.g., Brownlie and Taylor, 1981; Warrick and Mertes, 2009), discharge and suspended-sediment concentrations were compared to evaluate stationarity and time-dependent hysteresis patterns between these variables. Some computations were conducted for independent hydrologic 'events,' and, for the purposes here, unique 'events' were defined and separated by intervals of time with at least 48 h of continuous or decreasing stream discharge.

Hysteresis patterns in the relationships between stream discharge and sediment concentration were evaluated for each flow event if samples were adequately collected on both rising and falling limbs. Clockwise and counterclockwise hysteresis were defined to occur when at least an order-of-magnitude of difference in the concentrations were observed between equivalent streamflow rates during rising limb and falling limb samples. If concentrations varied less that an order of magnitude, the event was characterized as having 'no hysteresis.' Additionally, if the time-dependent patterns in concentration were greater than an order of magnitude for ranges of streamflow but these patterns did not follow a consistent hysteresis loop, the event was characterized as having a 'complex' pattern.

Each sediment concentration sample was classified into one of four subclasses based on discharge conditions (steady flow, rising limb, peak flow, or falling limb) using 5-h windows of streamflow measurements centered on each sample and using the following definitions:

(a) Rising limb: increase in discharge at a rate greater than 1 $m^3\,s^{-1}$ per hour.
(b) Peak flow: maximum flow of 5-h interval.
(c) Falling limb: decrease in discharge at a rate greater than 1 $m^3\,s^{-1}$ per hour.
(d) Steady flow: less than 1 $m^3\,s^{-1}$ per hour of discharge change in over interval.

Rates of increase in discharge were measured with the slopes from linear regression, and significance assessed at $p < 0.05$.

Suspended-sediment discharge was calculated by multiplying time-dependent stream discharge and suspended-sediment concentrations. These values were then corrected for the near-bed sampling bias (see Section 3.2 above) by multiplying by 0.87. This assumes a constant ratio between the flow-weighted and near-bed suspended-sediment concentrations across the watersheds and with time, which was consistent with the available data.

During high-flow events, it was common that each hourly discharge measurement had an independent suspended-sediment concentration measurement. For discharge records without sediment measurements, suspended-sediment concentrations were estimated in the following manner: (i) for time intervals with only one missing concentration between hourly discharge measurements (i.e., a one-record gap), the measurements before and after the missing concentration record were averaged; (ii) for time intervals longer than one hour, discharge-weighted suspended-sediment concentration estimates were generated using:

$$\mathrm{SSC}(t) = \mathrm{SSC}(t_0)\left(\frac{Q(t)}{Q(t_{0)}}\right)^{\mathrm{b}} \tag{1}$$

where SSC(t) is the suspended-sediment concentration at the time of interest (t), t_0 is the time of the last measured suspended-sediment concentration, Q is discharge, and b is the slope between the entire set of measured log(Q) and log(SSC) data, all of which are shown graphically in Fig. 2. This technique assumes that the concentrations were more likely to have 'memory' of the previously measured concentrations (i.e., at t_0) than changes that occurred following t, which is supported by time-dependent analysis results described below.

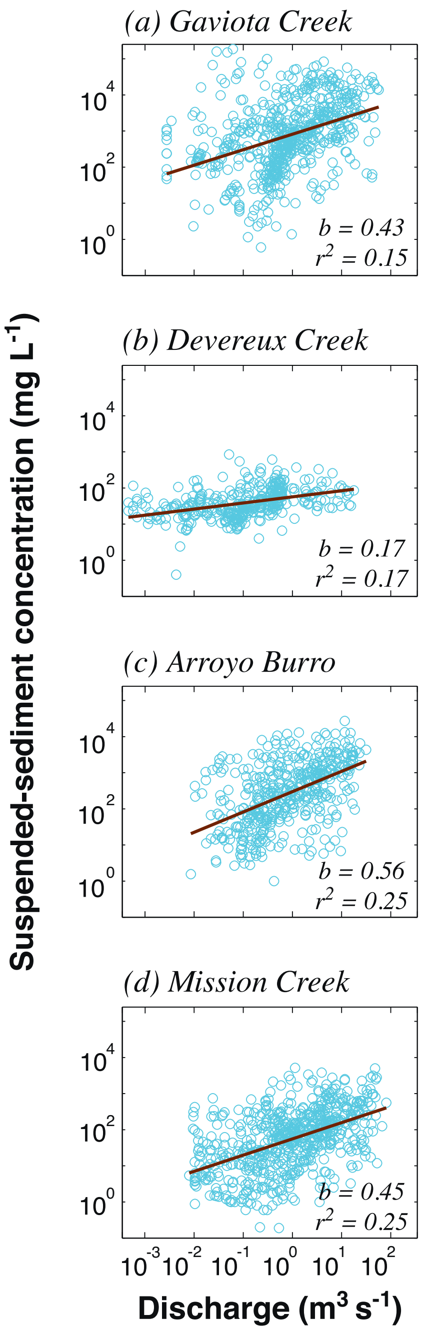

Fig. 2. The relationships between stream discharge and suspended-sediment concentration for the four study area watersheds, (a) Gaviota Creek, (b) Devereux Creek, (c) Arroyo Burro, and (d) Mission Creek. Lines represent the power-law regressions. Slopes (b) and correlation coefficients (r^2) of these regressions are also shown.

4. Results

4.1. Suspended-sediment concentrations

Measured suspended-sediment concentrations were only weakly related to stream discharge at the study area sites (Fig. 2). Linear regressions of the log-transformed discharge and sediment concentration data explained 15 to 25% of the variance in the concentration data, and there were at least order-of-magnitude differences in measured concentrations for the range of sampled discharge values. (Fig. 2). Sediment concentrations from Devereux Creek had a narrower range of

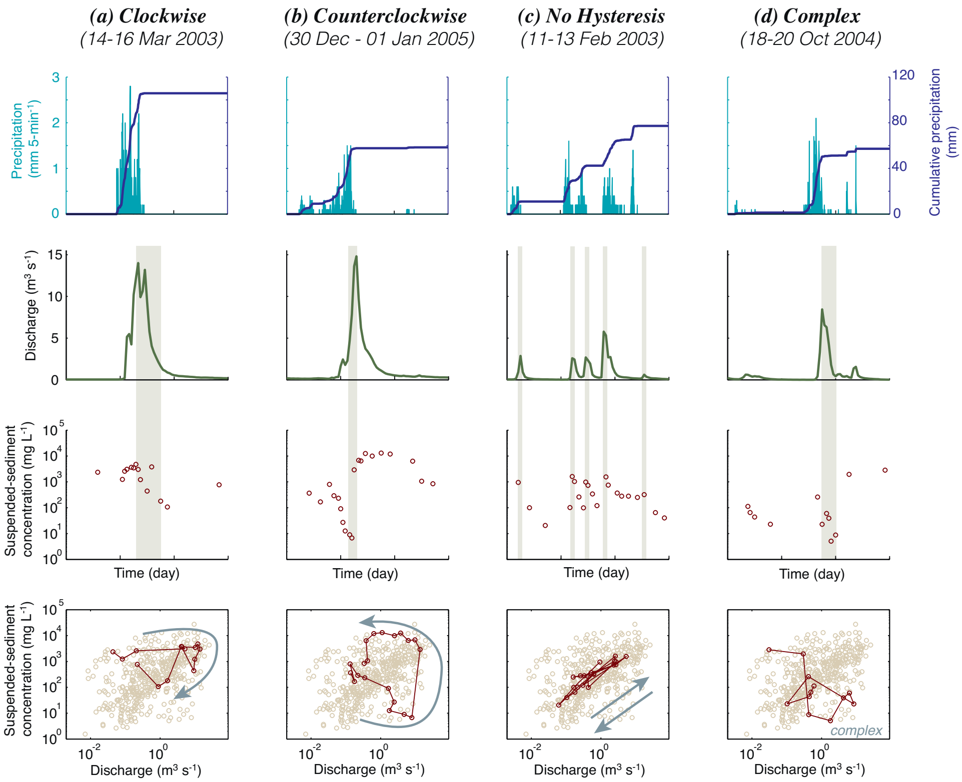

Fig. 3. Examples of suspended-sediment concentration dynamics during hydrologic events in Arroyo Burro to highlight the four time-dependent hysteresis patterns: (a) clockwise, (b) counter-clockwise, (c) no hysteresis, and (d) complex. The upper three panels show precipitation, discharge and sediment concentrations during four distinct 72-h intervals, and vertical bars in these plots highlight intervals of substantial change in sediment concentration. The bottom panel shows the relationships between discharge and sediment concentration during the event (dark symbols and line) and for the entire sample record (light symbols).

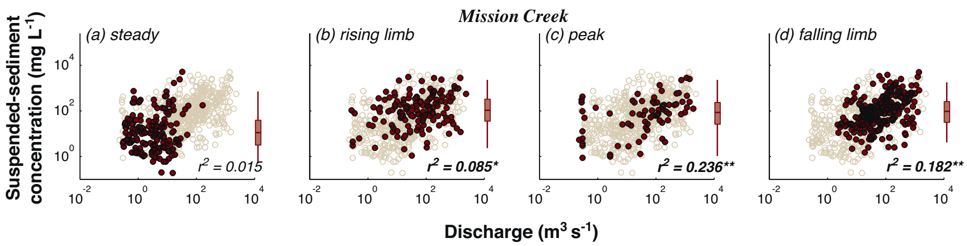

Fig. 4. The effect of sample collection timing on the discharge—suspended-sediment concentration relationships for Mission Creek. Sample data have been separated into four classes based on discharge conditions during the sampling: (a) steady, (b) rising limb, (c) peak, and (d) falling limb (see Methods for definitions). Correlation coefficients are shown for power-law regressions through each subset of data, and the statistical significance of these coefficients is denoted by: ** ($p < 0.00001$), * ($p < 0.05$), and no star ($p > 0.05$). Box plots on the right-hand side of each plot show the range in measured concentrations as computed by the median (line), interquartile range (box), and 2.5 and 97.5 percentiles (whiskers).

values that the other sites, and the maximum measured concentration in Devereux Creek was only 540 mg L^{-1}, compared to maxima of 5500–186,000 mg L^{-1} for the other three sites (Fig. 2).

High variance in suspended-sediment concentrations was common during high flow events, and different time-dependent hysteresis patterns were observed as shown, for example, by four Arroyo Burro events with similar peak discharge magnitudes (Fig. 3). The compilation of hysteresis observations suggested that 'complex' hysteresis patterns were the most common occurrence across the four watersheds (38–55% of observed events; Table 3). Clockwise or counterclockwise hysteresis was observed in 25–41% of the events depending on site, and there was a slightly greater abundance of counterclockwise events ($n = 25$) compared to clockwise events ($n = 16$) if all station data were combined (Table 3).

Additionally, measured suspended-sediment concentrations during the four distinct hydrologic conditions (steady, rising limb, peak, and falling limb) all revealed high variability in the discharge-concentration data (e.g., Mission Creek results shown in Fig. 4). Linear regressions of the log-transformed discharge and concentration data for each of these discharge conditions had low correlations ($r^2 = 0.002–0.33$ for all sites), and there is broad overlap in the range of concentrations

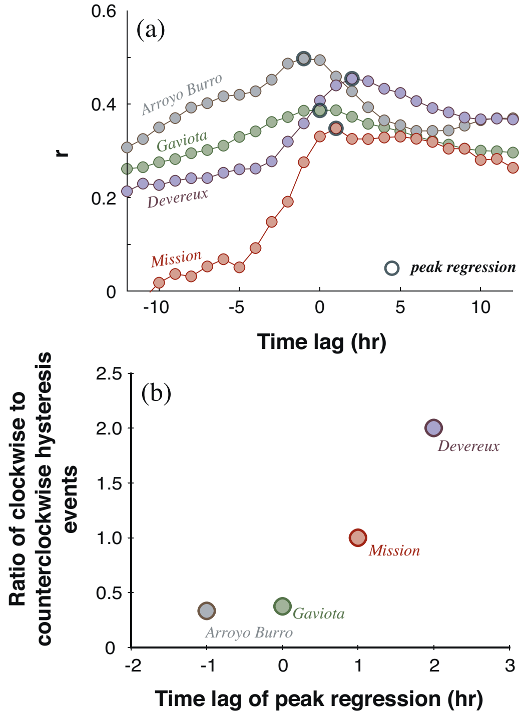

Fig. 5. (a) An assessment of time lag in the correlation coefficients (r) for power-law regressions between discharge and suspended-sediment concentration for the four study area creeks. Maximum correlations (highlighted symbols) are found for time lags within ±2 h. (b) Comparison of the time lag of maximum correlation and the ratio of measured clockwise to counterclockwise hysteresis events.

measured during each hydrologic condition (Fig. 4). The highest correlations between discharge and sediment concentration occurred either for peak discharge or rising limb samples, although these correlations were consistently low (r^2 = 0.24–0.33 for all sites). Sediment concentrations measured during 'steady' conditions were commonly lower than rising, peak or falling flow conditions (Fig. 4), and the lowest measured concentrations commonly occurred during the summer low-flow season.

Lagged regression analyses between discharge and measured sediment concentration revealed that peak correlations were found at between −1 and 2 h, and little difference was found between the correlation coefficients between unlagged and lagged regressions (Fig. 5a). Peak correlation coefficients (r) for these analyses ranged between 0.35 and 0.50, which are equivalent to r^2 of 0.12–0.25 (Fig. 5a). The results from the lagged correlations were consistent with the hysteresis analyses, such that stations with positive time lag had greater abundance of clockwise hysteresis events, and stations with negative lags had more counterclockwise events (Fig. 5b). Yet, although there was consistency in these results, the data revealed that discharge and suspended-sediment concentration were only weakly correlated and that these correlations were not better explained with simple rules of lag, hysteresis or flow-event separation (Figs. 2–5).

Monthly to annual time-dependent trends in the sampling results were evaluated from residuals in the log-transformed concentrations and the expected concentrations from least-squares power-law regressions through the data shown in Fig. 2. These residuals are equivalent to, and presented as, the ratios between the measured and expected concentrations, summarized in monthly percentiles (Fig. 6). Trends during each water year (October–September) were assessed by nonparametric Mann–Kendall tests ($p < 0.05$), although only three annual sampling intervals had significant trends: WY2005 in Gaviota Creek, WY2004 in Devereux Creek, and WY2004 in Mission Creek (Fig. 6). All of these significant time-dependent trends were sloped downward with time, which suggests decreases in sediment concentrations with respect to discharge over the water year. The greatest decreasing slope and most significant results occurred for Gaviota Creek during the water year following a wildfire (Kendall tau = -0.24; $p < 10^{-11}$), during which median concentrations decreased by ~100 fold from the expected concentrations between October 2004 and May 2005 (Fig. 6a). Following this decrease in WY2005, suspended-sediment concentrations in Gaviota Creek remained lower than those measured immediately following the wildfire. No other statistically significant multi-year trends were found in suspended-sediment concentrations for the study sites.

4.2. *Suspended-sediment discharge and yield*

Suspended-sediment discharge varied greatly during the high flow events of the winter season. For example, suspended-sediment discharge rates in Gaviota Creek during a 8-day event with several pulses of discharge are shown in Fig. 7. Although this record characterizes three distinct peak flows with discharge equal to or greater than 10 $m^3 s^{-1}$, suspended-sediment

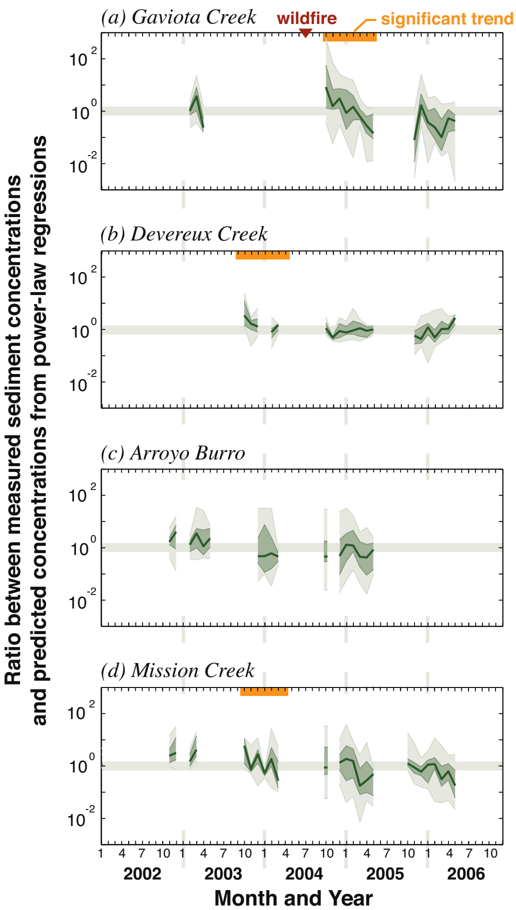

Fig. 6. Time-dependent changes in the discharge-suspended sediment concentration relationships as shown by the ratios between measured concentrations and predicted concentration from power-law regressions shown in Fig. 2 for the four study area watersheds: (a) Gaviota Creek, (b) Devereux Creek, (c) Arroyo Burro, and (d) Mission Creek. Data shown include the monthly median (dark line), interquartile range (dark shading) and the range in values (light shading). Water years with orange bars have significant decreasing time-dependent residuals ("significant trend") during the winter seasons as determined by Mann–Kendall tests ($p < 0.05$). No increasing trends were observed for any of the stations during any of the years.

Table 4
Comparison of suspended-sediment yields from the study area watersheds during four water years (WY).

	Gaviota Cr.	Devereux Cr.	Arroyo Burro	Mission Cr.
Sediment discharge (t yr^{-1}):				
WY 2003	2800	n.a.	2500	1570
WY 2004	n.a.	61	400	141
WY 2005	108,000	135	17,400	10,000
WY 2006	6000	86	n.a.	650
Sediment yield (t km^{-2} yr^{-1}):				
WY 2003	53	n.a.	100	52
WY 2004	n.a.	6.3	15.7	4.7
WY 2005	2100	14.1	680	340
WY 2006	117	9.0	n.a.	22

discharge during these three high flows was markedly different largely owing to differences in suspended-sediment concentrations (Fig. 7c). Thus, the majority of the sediment discharged during the 8-day interval of time occurred during just two of these three higher flows (vertical shading; Fig. 7).

Similar suspended-sediment discharge computations were made for all four of the studied watersheds, and high spatial and temporal variability in sediment discharge and yield were found. For example, Devereux Creek was found to have relatively stable annual sediment yields during three years of observations (6.3 to 14 t km^{-2} yr^{-1}; Fig. 8, Table 4). This is in contrast to the high temporal variability in the other three sites, as exhibited by 1–2 order-of-magnitude differences in annual sediment yields (4.7–2100 t km^{-2} yr^{-1}; Fig. 8). The largest annual sediment yield was 2100 t km^{-2} yr^{-1} measured

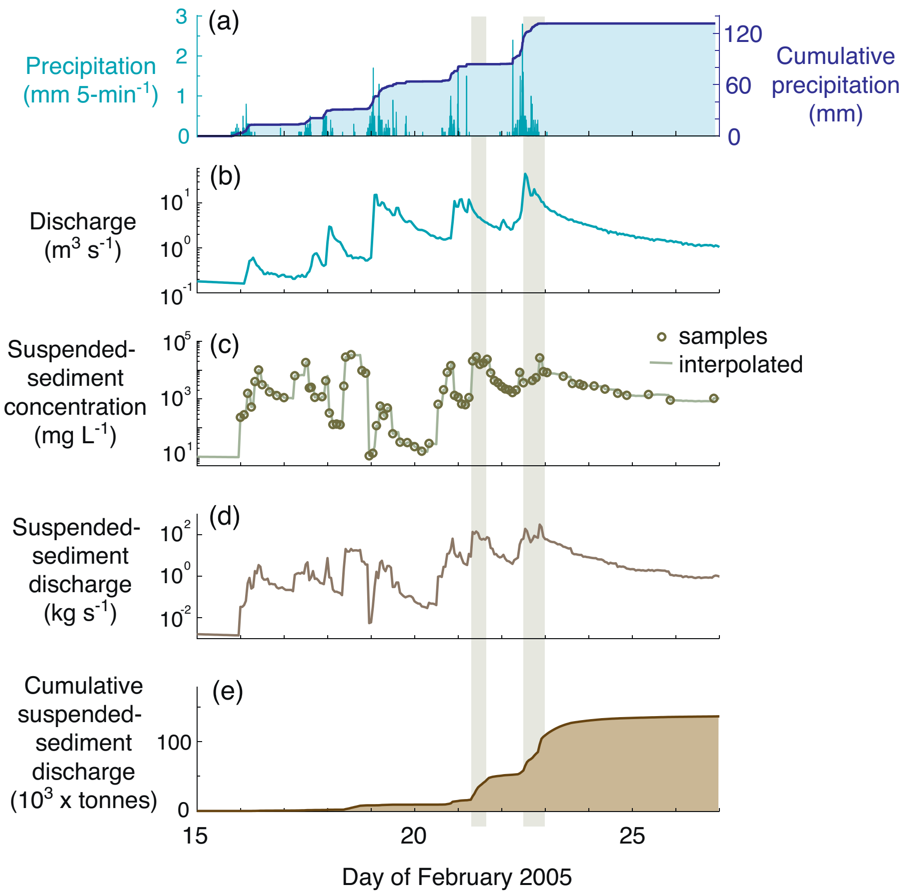

Fig. 7. An example of the hydrologic forcing and response of Gaviota Creek during a hydrologic event, including (a) precipitation, (b) stream discharge, (c) measured and interpolated near-bed suspended-sediment concentrations, and (d) instantaneous and (e) cumulative suspended-sediment discharge from measurements of stream discharge and suspended-sediment concentrations and the flow-weighted correction factor. These data provide an example of the temporal frequency of sampling and the high variability in discharge and sediment concentrations during events. Two intervals of time with the highest rates of sediment discharge are highlighted with vertical bars.

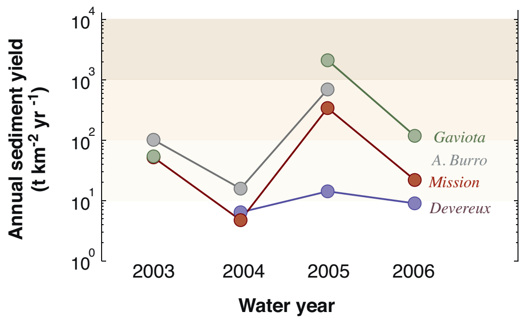

Fig. 8. Annual suspended-sediment yields measured for the four study area watersheds.

during WY2005 for Gaviota Creek, which as noted above occurred following a partial burn of this watershed by wildfire that significantly raised sediment concentrations.

These computations also provided information about the total increment of time during each hydrologic year that various suspended-sediment concentrations were met or exceeded. The only water year with sediment discharge records for all four watersheds was WY2005, so we focus on a comparison of these results. Time-weighted suspended-sediment concentrations from the four watersheds during WY2005 are compared in Fig. 9, and these values have been corrected for the near-bed sample bias. Median suspended-sediment concentrations during the year ranged between 0.8 and 18 mg L^{-1}, the lowest of these was observed in Mission Creek (Fig. 9). Although Devereux had the highest median sediment concentration (18 mg L^{-1}),

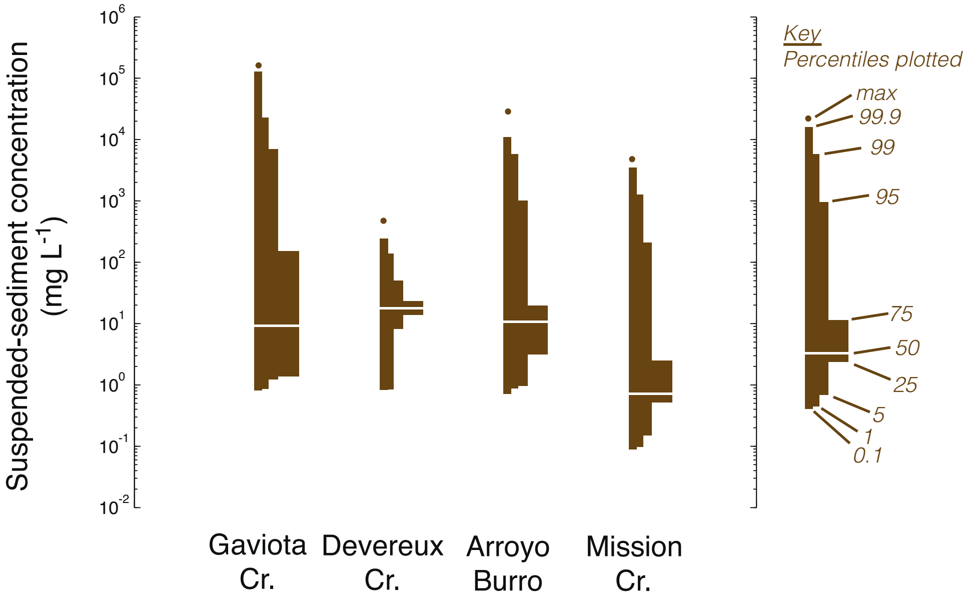

Fig. 9. A comparison of the time-weighted suspended-sediment concentrations for the four study area creeks during water year 2005. The histograms shown are for flow-weighted concentrations, which have been derived from the near-bed concentrations using the bias correction of 0.87.

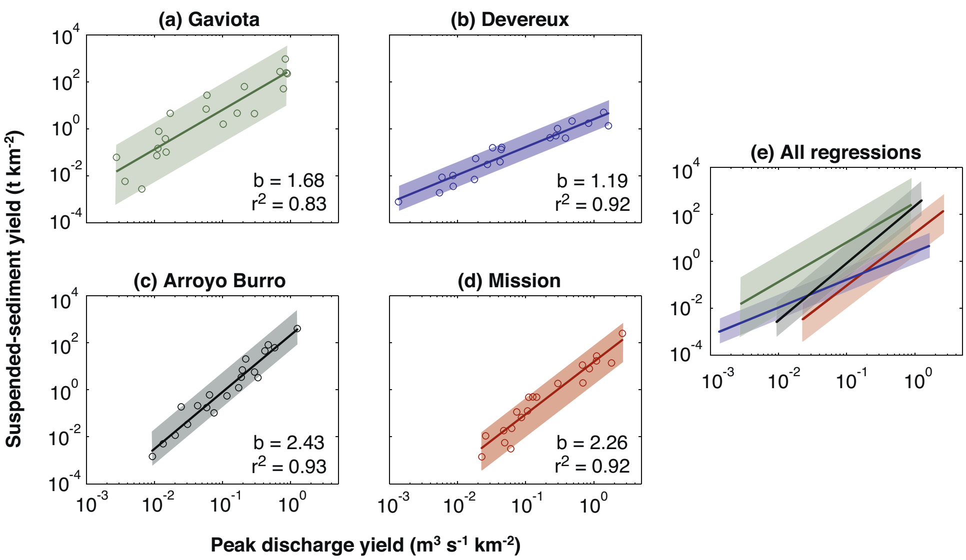

Fig. 10. Comparisons of the relationships between peak water discharge yield and total suspended-sediment discharge yield for the study area watersheds during hydrologic events of water year 2005: (a) Gaviota Creek, (b) Devereux Creek, (c) Arroyo Burro, and (d) Mission Creek. Power-law regressions and the range of data about these regressions shown with line and shading, respectively. Slopes (b) and correlation coefficients (r^2) of these regressions are also shown. The regression lines and shading from (a)–(d) are combined in (e).

this watershed generated the lowest peak suspended-sediment concentration (470 mg L^{-1}), which was one to several orders-of-magnitude lower than the peak concentrations of the other creeks (Fig. 9). There are also fundamental differences in the shapes of the sediment concentration frequency distributions; Devereux had a narrow distribution with little skew in log-transformed data (Fig. 9). In contrast, the three other watersheds (Gaviota, Arroyo Burro, and Mission) had strongly skewed distributions toward the maximum measured concentrations (Fig. 9).

Suspended-sediment discharge was generally related to the size of the hydrologic event, as shown by event-based comparisons of sediment yield and peak stream discharge (Fig. 10). For comparative purposes, sediment discharge and peak discharge values during each event have been normalized by watershed areas to generate hydrologic “yields” in Fig. 10. The greatest scatter between peak discharge and sediment discharge occurred for Gaviota Creek (r^2 = 0.83; Fig. 10), which, as noted above, had significant time-dependent trends in suspended-sediment concentrations during WY2005 following a

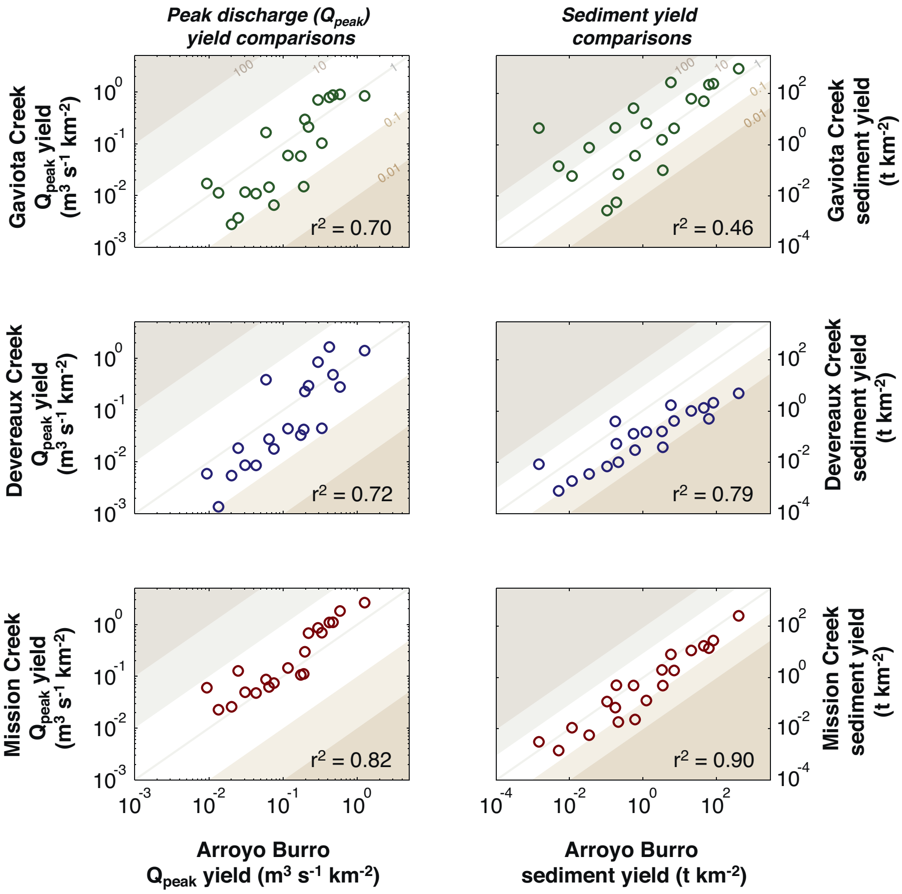

Fig. 11. Inter-comparisons of peak water discharge yield and total suspended-sediment discharge yield across the study area watersheds during hydrologic events of water year 2005. Comparisons are made against Arroyo Burro, and shading represents order-of-magnitude differences between the yields during events.

wildfire (Fig. 6a). Data from the three other watersheds had correlation coefficients (r^2) greater than 0.92 and less scatter about the fitted regression than found for Gaviota Creek (Fig. 10). One substantial difference among the watersheds was the power-law regression slopes, which were higher for Arroyo Burro and Mission creeks ($b > 2$) than for Gaviota Creek ($b = 1.7$) or Devereux Creek ($b = 1.2$; Fig. 10). Although Arroyo Burro and Mission Creek had similar regression slopes, these regression lines were offset by an order of magnitude (Fig. 10e), which was consistent with the order-of-magnitude differences in suspended-sediment concentrations (Fig. 9).

The observed differences in the peak discharge–suspended-sediment yield relationships were related to non-constant rates of stream discharge and sediment yield. For example, peak discharge yields across the study area were correlated at $r^2 = 0.70–0.82$ (power law; Fig. 11; Arroyo Burro is used for comparative purposes because it consistently resulted in the best correlations with the other watersheds), and peak discharge yields differed by over 10-fold for some events. Similarly, sediment yields across the study area watersheds had wide ranging correlations ($r^2 = 0.46–0.90$, power law; Fig. 11), and differences in these yields during any one high flow event could exceed 100-fold. The Devereux Creek sediment yields were measurably lower than the other watersheds during the majority of events, and were especially lower for the events with the highest peak discharge rates (Fig. 11).

Precipitation was also found to correlate significantly with event-based sediment yields. For example, total precipitation measured during the event could explain between 72 and 84% of the event-based sediment yield variance (Fig. 12). These correlations did not improve if total precipitation was replaced with the maximum precipitation intensity over any interval of time (Fig. 13a). It was observed, however, that the peak rainfall intensity over 0.5 to 1 h provided the best correlations, even if these correlations were not greater than those found for total precipitation (Fig. 13a). Additionally, analyses that assessed whether pre-event precipitation significantly influenced sediment yields resulted in limited evidence of an effect. For example, including preceding days in the total precipitation calculations improved correlation coefficients (r^2) for Gaviota Creek from 0.72 to 0.82 (peak found for 9 preceding days; Fig. 13b). However, Arroyo Burro and Mission Creek did not show this effect, and there was a very moderate effect found in Devereux Creek (Fig. 13b).

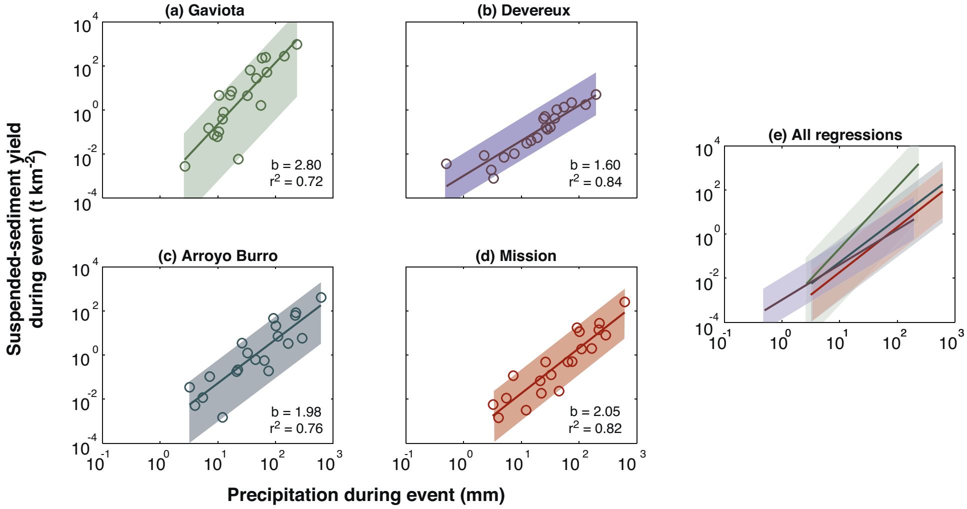

Fig. 12. Comparisons of the relationships between event precipitation and total suspended-sediment discharge yield for the study area watersheds during hydrologic events of water year 2005: (a) Gaviota Creek, (b) Devereux Creek, (c) Arroyo Burro, and (d) Mission Creek. Power-law regressions and the range of data about these regressions shown with line and shading, respectively. Slopes (*b*) and correlation coefficients (r^2) of these regressions are also shown. The regression lines and shading from (a)–(d) are combined in (e).

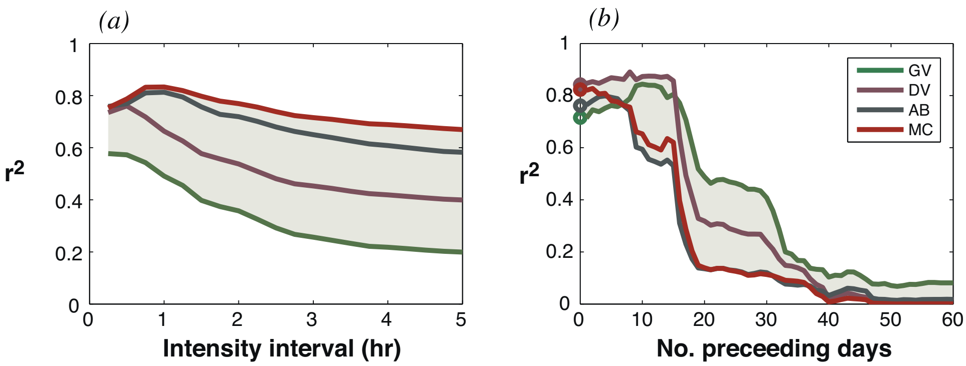

Fig. 13. An evaluation of precipitation intensity and preceding precipitation on the suspended-sediment discharge yield for the study area watersheds during hydrologic events of water year 2005. (a) Correlation coefficients for power-law regressions between maximum precipitation intensity over 0.25 to 5 h increments during each event and suspended-sediment discharge yield. All coefficients are lower than those shown in Fig. 12. (b) Correlation coefficients for power-law regressions between total precipitation during event and a varying number of preceding days before the event. Peak correlations occur for 0 to 9 preceding days.

5. Discussion

5.1. Comparison of results

Hydrologic monitoring of several Santa Ynez Mountain creeks resulted in the characterization of suspended-sediment discharge patterns and trends during several water years. Important similarities and differences were found in the sediment discharge characteristics among these watersheds. A primary similarity is that water and sediment discharge were ephemeral and dominated by rainfall-generated high flows. For example, using discharge information from WY2005 it can be shown that the majority of water and sediment discharge for all the study sites occurred during a small fraction of time. Half of all suspended-sediment discharged occurred during a cumulative 0.5–2 days during the year, and half of the water discharged occurred during a cumulative 3–7 days (Fig. 14). These results are consistent with longer records from larger rivers in the southern California (Warrick and Milliman, 2003) and other small watersheds in semi-arid regions throughout the world (e.g., Coppus and Imeson, 2002; Rustomji and Wilkinson, 2008; Duvert et al., 2011, 2012; Conaway et al., 2013; Gray et al., 2015), which show that infrequent events produce the majority of water and sediment discharge from these watersheds.

The ephemeral nature of sediment discharge across the study area is complex, however, owing to irregular patterns in the suspended-sediment concentrations. Not only is there high variability in the discharge—sediment concentration relationships across the study area (Fig. 2), but these relationships can also have multiple time-dependent forms over the course of hydrologic events (Fig. 3). The majority of sediment discharge occurred when both stream discharge and sediment

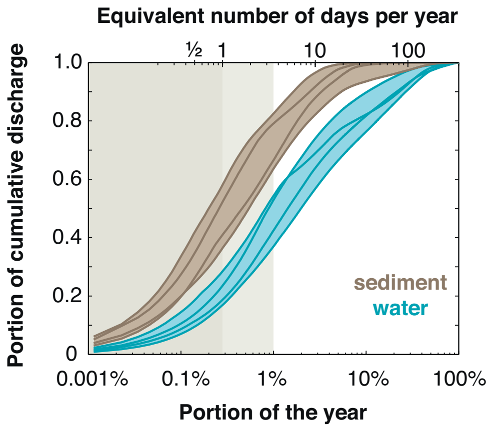

Fig. 14. Comparison of the flux-frequency relationships for the cumulative water and suspended-sediment discharge from the study area watersheds during water year 2005. Roughly half of the suspended sediment discharged from the watersheds consistently occurred in ~1 day during the year.

concentrations were elevated (Fig. 7), the latter of which could reach 10,000s to over 100,000 mg L^{-1} during high flow events, levels that are several orders of magnitude greater than median concentrations during the water year (Fig. 9). These findings are consistent with many of the small watersheds in the headlands of semiarid regions of the world (e.g., Lenzi and Marchi, 2000; Seeger et al., 2004; Zabaleta et al., 2007; Polyakov et al., 2010). This high variability in suspended-sediment discharge is largely attributed to the highly variable and stochastic nature of sediment supply in the landscape and channels of these steep, small watersheds.

Empirical analyses have provided evidence that over scales of dozens of hydrologic events, sediment yields in these small steep watersheds may be related to water discharge yields (e.g., Tropeano, 1991; Rankl, 2004; Polyakov et al., 2010; Duvert et al., 2012; Gao et al., 2013). Our results support these findings for three of the four watersheds (Fig. 10). One watershed, Gaviota Creek, did not fit this model well, largely owing to increases in sediment supply related to a wildfire (Fig. 6). This provides a cautionary tale about empirical models of peak discharge and sediment yield, which may change with time after large sediment supply events from wildfire, earthquakes, landslides or human impacts (*cf.* Trimble, 1997; Dadson et al., 2004; Shakesby and Doerr, 2006; Warrick and Rubin, 2007; Hovius et al., 2011; Warrick et al., 2013a; García-Ruiz et al., 2013).

While there were several similarities across the studied watersheds, there were also several substantial differences. The greatest difference among the watersheds was the lower sediment concentrations and sediment yields measured in Devereux Creek compared to the other sites (Table 4; Figs. 2, 9, 11). During the wet 2005 water year, the sediment yield of Devereux Creek was several orders of magnitude lower than the other sampled sites (*cf.* Tables 1 and 4). These differences are likely related to different watershed characteristics in Devereux Creek–such as relief, slope, land cover, and lithology–compared to the other well-studied Santa Ynez Mountain watersheds that drain steeper and higher elevation landscape up to the crest of the mountain range (Table 2). Furthermore, Devereux Creek was the most urbanized of the watersheds studied, and also had a substantial area modified for rangeland and agricultural practices (Table 2) which likely modified water and sediment discharge properties (e.g., Trimble, 1997; Konrad and Booth, 2005). Regardless of the cause, it was clear that the sediment discharge properties for this lowland urban creek were substantially different than the adjacent steep mountainous creeks that have formed the basis of most sediment yield studies in the region (Table 1). Thus, it is likely that the steepest landscapes in the region provide the dominant supply of sediment (*cf.* Tropeano, 1991), and that simple estimation techniques such as assumptions of constant sediment yields would result in erroneous results if used across the broader region of the Santa Barbara coastal watersheds.

Subtler, but equally important, differences were observed in the adjacent and similar Arroyo Burro and Mission Creek watersheds. For example, suspended-sediment concentrations for these two watersheds differed by approximately an order of magnitude (Fig. 9). Similarly, event-based sediment discharge relationships differed by about an order of magnitude (Fig. 10). These differences were partially compensated for by higher river discharge rates in Mission Creek (Fig. 11), such that the ratio of Arroyo Burro to Mission Creek sediment yield was 1.9–3.3 for the three comparative water years (Table 4).

5.2. Assessment of sediment yield estimation methods

Because there are coastal regions throughout the world that are lined with small watersheds for which little, if any, information exists about material fluxes (Fig. 1a), there is need to develop techniques to estimate loads for these regions. In this study we were able to examine several different techniques that may be used estimate material loads or extrapolate load information from one watershed to another. Here we provide a brief summary of these techniques and provide assessments, using our data, for the potential application of each technique.

Sediment rating curves are techniques that utilize relationships between river sediment concentrations and streamflow to extend sediment load observations from a series of samples to long, continuous intervals of time without samples (Asselman, 2000; Horowitz, 2003; Warrick, 2014). Unfortunately, streamflow could not be used to explain much of the variability of sediment concentrations in the study area watersheds, even if time-varying patterns such as hysteresis or lags were included (Figs. 2–6). This makes sediment-rating curves a poor sediment discharge estimation technique for watersheds like those found in our study area. Rating-curve relationships have been successfully developed and used for larger watersheds (O(1000 km^2)) of the California region (Brownlie and Taylor, 1981; Warrick and Mertes, 2009), for which sediment loads have been assumed to be less variable with time. However, for the O(10 km^2) watersheds studied here, sediment rating curves would provide poor results.

The use of hydrologic metrics, such as peak streamflow or precipitation rates, may also be used to develop estimates of sediment discharge from small watersheds such as those studied here (Duvert et al., 2012; Gao et al., 2013). We found that these hydraulic metrics were strongly correlated with sediment yields across numerous events (Figs. 10 and 12), which provides support for the use of these techniques. There was not a universal relationship between peak streamflow yield and sediment yield across the four study sites, however, which suggests that these relationships may not be extrapolated from one watershed to another (10). Precipitation provided a more consistent relationship with sediment yield and may provide a better means for estimating sediment yields for our study area (Fig. 12e).

A simpler approach is to assume that measured sediment yields, whether measured over individual events or several year records, are relatively equivalent, and hence transferable from monitored to unmonitored basins (Milliman and Farnsworth, 2011). A comparison of Devereux and Gaviota Creeks should provide caution to the use of this simple approach. The former site produced fairly stable sediment yields year-to-year, unlike the remaining watersheds (Fig. 14; Table 4). These patterns are consistent with the characteristics of this watershed (lower elevation, lesser slope, more urbanized; Table 2), although a rigorous statistical evaluation of watershed properties is not possible with the data presented here. The sediment yield of the Gaviota Creek site, in contrast, had strong time-dependencies that were consistent with the effects of wildfire within part of its watershed (Figs. 6 and 14). Thus, there can be watershed conditions that cause nonlinear or time-dependent relationships in sediment yields. Any technique developed to extend or estimate sediment yields from unmonitored coastal basins such as those studies here will need to include these kinds of effects.

5.3. *Application to global sediment yields.*

Over the global scale it is suggested that sediment yield (SY) and watershed area (A) are related by SY$\sim A^{-0.5}$ (Syvitski and Milliman, 2007). Because the global database used to develop this relationship did not have watersheds smaller than 100 km^2, it is relevant to inquire whether the strong area-dependence extends to the O(10 km^2) watersheds studied here. Sediment yields for the broader western Transverse Ranges of our study area have been reported to be 740–5300 t km^{-2} yr^{-1} from watersheds that averaged 1200 km^2 in drainage area (Warrick and Mertes, 2009). Applying the Syvitski and Milliman (2007) relationship to these results, the Santa Ynez Mountain watersheds, which average roughly 30 km^2, should have sediment yields that range 4700–34,000 t km^{-2} yr^{-1}. These estimated values surpass measured annual sediment yields even following the exceptional erosion that occurs following wildfires (Table 1).

This suggests that the strong watershed-area dependence derived from global sediment yields (Syvitski and Milliman, 2007), likely do not extend through watershed sizes less than ∼1000 km^2. This is consistent with sediment yields from debris basin sedimentation of watersheds sized 0.2–18 km^2 throughout the western Transverse Ranges, which were found to correlate with $A^{-0.172}$ to $A^{0.132}$ (Scott and Williams, 1978; their Eqs. (1)–(3)). Combined, this suggests that sediment inventories should not extend the strong SY$\sim A^{-0.5}$ relationship through the smallest coastal watersheds of the world, especially for high sediment yield regions such as the coastal California area studied here.

6. Conclusions

Several small watersheds of the Santa Ynez Mountains were monitored to characterize the patterns and trends of suspended-sediment discharge from watershed types that are generally underrepresented in global geochemical databases. These watersheds produced highly variable rates of sediment discharge that were punctuated by infrequent events with suspended-sediment concentrations that could reach and exceed 100,000 mg L^{-1}. The high temporal and spatial variability in watershed sediment supply and discharge makes the utility of calculation methods, such as sediment rating curves (e.g., Asselman, 2000; Horowitz, 2003) and extrapolation of measured sediment yields to unmonitored basins (e.g., Milliman, 1995; Duvert et al., 2012), inadequate techniques for these small watersheds. This suggests that sediment supply models developed for headwater watersheds (e.g., Duvert et al., 2012) should be used with caution to fill significant gaps in global sediment discharge inventories owing to the likelihood for high variability – in both time and space – of actual sediment yields. Furthermore, sufficient care should be taken to include the potential effects of rare, infrequent events such as earthquakes, wildfires and floods (García-Ruiz et al., 2013) that may disrupt and significantly alter sediment yields of these small watersheds over time. These conclusions emphasize the importance of initiating, continuing and renewing sampling programs (e.g., Duvert et al., 2011) to characterize sediment and geochemical yields from the small coastal watersheds of the world.

Conflict of interest

None.

Acknowledgements

This work was supported by the Santa Barbara Coastal Long-Term Ecological Research project, funded by the National Science Foundation (OCE-9982105 and OCE-0620276). We thank F. Setaro, A. Doyle, and undergraduate assistants for laboratory analyses and A. Leydecker, S. Coombs, T. Robinson, and undergraduate assistants for sample collection. B. Goodridge received additional financial support from the Henry Luce Foundation, and J. Warrick was supported by the USGS Coastal and Marine Geology Program.

Appendix A. Supplementary data

Supplementary data associated with this article can be found, in the online version, at http://dx.doi.org/10.1016/j.ejrh.2015.08.004.

References

Asselman, N.E.M., 2000. Fitting and interpretation of sediment rating curves. J. Hydrol. 234, 228–248.
Beusen, A.H.W., A.L.M. Dekkers, A.F., Bouwman, W. Ludwig, and J. Harrison, 2005, Estimation of global river transport of sediments and associated particulate C, N, and P. Global Biogeochemical Cycles, v. 19, GBS05.
Beighley, R.E., Melack, J.M., Dunne, T., 2003. Impacts of California's climatic regimes and coastal land use change on streamflow characteristics. J. Am. Water Resour. Assoc. 39 (6), 1419–1433.
Brownlie, W.R., Taylor, B.D., 1981. Sediment Management for Southern California Mountains, Coastal Plains and Shoreline; Part C. Coastal Sediment Delivery by Major Rivers in Southern California. California Institute of Technology Environmental Quality Laboratory Report No. 17-C, Pasadena, California314.
Brzezinski, M.A., Reed, D.C., Harrer, S., Rassweiler, A., Melack, J.M., Goodridge, B.M., Dugan, J.E., 2013. Multiple sources and forms of N sustain year-round kelp growth on the inner continental shelf of the Santa Barbara channel. Oceanography 26, 114–123.
Cole, K.L., Liu, G.W., 1994. Holocene paleoecology of an estuary on Santa Rosa Island, California. Quat. Res. 41, 326–335.
Conaway, C.H., Draut, A.E., Echols, K.R., Storlazzi, C.D., Ritchie, A., 2013. Episodic suspended sediment transport and elevated polycyclic aromatic hydrocarbon concentrations in a small, mountainous river in coastal California. River Res. Appl. 29, 919–932.
Coombs, J.S., Melack, J.M., 2012. The initial impacts of a wildfire on hydrology and suspended sediment and nutrient export in California chaparral watersheds. Hydrol. Processes, http://dx.doi.org/10.1002/hyp.9508.
Coppus, R., Imeson, A.C., 2002. Extreme events controlling erosion and sediment transport in a semi-arid sub-Andean valley. Earth Surface Processes Landforms 27, 1365–1375.
Clark, S.E., Siu, Y.S., Pitt, R., Roenning, C.D., Treese, D.P., 2009. Peristaltic pump autosamplers for solids measurement in stormwater runoff. Water Environ. Res. 81 (2), 192–200.
Croll, D.A., Marinovic, B., Benson, S., Chavez, F.P., Black, N., Ternullo, R., Tershy, B.R., 2005. From wind to whales: trophic links in a coastal upwelling system. Mar. Ecol. Prog. Ser. 289, 117–130.
Dadson, S.J., Hovius, N., Chen, H., Dade, W.B., Lin, J.-C., Hsu, M.-L., Lin, C.-W., Horng, M.-J., Chen, T.-C., Milliman, J.D., Stark, C.P., 2004. Earthquake-triggered increase in sediment delivery from an active mountain belt. Geology 32 (8), 733–736.
de Vente, J., Verduyn, R., Verstraeten, G., Vanmaercke, M., Poesen, J., 2011. Factors controlling sediment yield at the catchment scale in NW Mediterranean geoecosystems. J. Soils Sediments 11, 690–707.
Duggins, D.O., Simenstad, C.A., Estes, J.A., JA, 1989. Magnification of secondary production by kelp detritus in coastal marine ecosystems. Science 245 (4914), 170–173.
Duvall, A., Kirby, E., Burbank, D., 2004. Tectonic and lithologic controls on bedrock channel profiles and processes in coastal California. J. Geophys. Res. 109, F03002.
Duvert, C., Gratiot, N., Némery, J., Burgos, A., Navratil, O., 2011. Sub-daily variability of suspended sediment fluxes in small mountainous catchments-implications for community-based river monitoring. Hydrol. Earth Syst. Sci. 15, 703–713, http://dx.doi.org/10.5194/hess-15-703-2011.
Duvert, C., Nord, G., Gratiot, N., Navratil, O., Nadal-Romero, E., Mathys, N., Némery, J., Regüés, D., García-Ruiz, J.M., Gallart, F., Esteves, M., 2012. Towards prediction of suspended sediment yield from peak discharge in small erodible mountainous catchments (0.45–22 km^2) of France Mexico and Spain. J. Hydrol. 454–455, 42–55.
Ejarque, A., Anderson, R.S., Simms, A.R., Gentry, B.J., 2015. Prehistoric fires and the shaping of colonial transported landscapes in southern California: a paleoenvironmental study at Dune Pond, Santa Barbara County. Quat. Sci. Rev. 112, 181–196.
Farnsworth, K.L., Warrick, J.A., 2007. Sources, Dispersal, and Fate of Fine Sediment Supplied to Coastal California. U.S. Geological Survey77 p, Scientific Investigations Report 2007–5254.
Florsheim, J.L., Keller, E.A., Best, D.W., 1991. Fluvial sediment transport in response to moderate storm flows following chaparral wildfire, Ventura County, Southern California. Geol. Soc. America Bull. 103, 504–511.
Foley, M.M., Koch, P.L., 2010. Correlation between allochthonous subsidy input and isotopic variability in the giant kelp *Macrocystis pyrifera* in central California, USA. Mar. Ecol. Prog. Ser. 409, 41–50.
Gabet, E.J., Dunne, T., 2002. Landslides on coastal sage scrub and grassland hillslopes in a severe El Niño winter: The effects of vegetation conversion on sediment delivery. Geol. Soc. Am. Bull. 114, 983–990.
Galewsky, J., Stark, C.P., Dadson, S., Wu, C.C., Sobel, A.H., Horng, M.J., 2006. Tropical cyclone triggering of sediment discharge in Taiwan. J. Geophys. Res. 111, F03014.
Gao, P., Nearing, M.A., Commons, M., 2013. Suspended sediment transport at the instantaneous and event time scales in semiarid watersheds of southeastern Arizona, USA. Water Resour. Res. 49, 6857–6870, http://dx.doi.org/10.1002/wrcr.20549.
García-Ruiz, J.M., Ndala-Romero, E., Lana-Renault, N., Beguería, S., 2013. Erosion in Mediterranean landscapes: changes and future challenges. Geomorphology 198, 20–36.
Gomez, B., Trustrum, N.A., Hicks, D.M., Rogers, K.M., Page, M.J., Tate, K.R., 2003. Production, storage, and output of particulate organic carbon: Waipaoa River basin, New Zealand. Water Resour. Res. 36, 1161, http://dx.doi.org/10.1029/2002WR001619.
Goodridge, B.M., Melack, J.M., 2012. Land use control of stream nitrate concentrations in mountainous coastal California watersheds. J. Geophys. Res. 117, G02005.
Graft, W.L., 1988. Fluvial Processes in Dryland Rivers. Springer-Verlag, Berlin.

Gray, A.B., Pasternack, G.B., Watson, E.B., Warrick, J.A., Goñi, M.A., 2015. Effects of antecedent hydrologic conditions, time dependence, and climate cycles on the suspended sediment load of the Salinas River, California. J. Hydrol. 525, 632–649.
Grodek, T., Jacoby, Y., Morin, E., Katz, O., 2012. Effectiveness of exceptional rainstorms on a small Mediterranean basin. Geomorpholgy 159–160, 156–168.
Gurnell, A.M., Clark, M.J., Hill, C.T., Greenhalgh, J., 1992. Reliability and representativeness of a suspended sediment concentration monitoring programme for a remote alpine proglacial river. IAHS Publication no. 210.
Guy, H.P., Norman, V.W., 1970. Field methods for measurement of fl uvial sediment, in Techniques of Water-Resources Investigations. In: Book 3. Applications of Hydraulics. U.S. Government Printing Office, Washington D.C, pp. 59 p.
Hill, B.R., and McConaughy, C.E., 1988, Sediment loads in the Ventura River Basin, Ventura County, California, 1969-81: U. S. Geological Survey Water-Resources Investigations Report 88-4149. Sacramento, CA., 22 p.
Hinderer, M., Kastowski, M., Kamelger, A., Bartolini, C., Schlunegger, F., 2013. River loads and modern denudation of the Alps—a review. Earth-Sci. Rev. 118, 11–44.
Horowitz, A.J., 2003. An evaluation of sediment rating curves for estimating suspended sediment concentrations for subsequent flux calculations. Hydrol. Processes 17 (17), 3387–3409.
Horowitz, A.J., Rinella, F.A., Lamothe, P., Miller, T.L., Edwards, T.K., Roche, R.L., Rickert, D.A., 1990. Variations in suspended sediment and associated trace element concentrations in selected riverine cross sections. Environ. Sci. Technol. 24, 1313–1320.
Hovius, N., Meunier, P., Lin, C.W., Chen, H., Chen, Y.G., Dadson, S., Horng, M.J., Lines, M., 2011. Prolonged seismically induced erosion and the mass balance of a large earthquake. Earth Planet. Sci. Lett. 304 (3), 347–355.
Inman, D.L., Jenkins, S.A., 1999. Climate change and the episodicity of sediment flux of small California rivers. J. Geol. 107, 251–270.
Keller, E.A., Valentine, D.W., Gibbs, D.R., 1997. Hydrological response of small watersheds following the southern California painted cave fire of June 1990. Hydrol. Processes 11, 401–414.
Konrad, C.P., Booth, D.B., 2005. Hydrologic changes in urban streams and their ecological significance. Am. Fish. Soc. Symp. 47, 157–177.
Lamb, M.P., Scheingross, J.S., Amidon, W.H., Swanson, E., Limaye, A., 2011. A model for fire-induced sediment yield by dry ravel in steep landscapes. J. Geophys. Res.-Earth Surf. 116 (3), F0300.
Lavé, J., Burbank, D.W., 2004. Denudation processes and rates in the Transverse Ranges, southern California: erosional response of a transitional landscape to external and anthropogenic forcing. J. Geophys. Res.-Earth Surf. 109, F01006.
Lenzi, M.A., Marchi, L., 2000. Suspended sediment load during floods in a small stream of the Dolomites (northeastern Italy). Catena 39 (4), 267–282.
Ludwig, W., Dumont, E., Meybeck, M., Heussner, S., 2009. River discharges of water and nutrients to the Mediterranean and Black Sea: Major drivers for ecosystem changes during past and future decades? Prog. Oceanogr. 80 (3–4), 199–217.
Luyendyk, B.P., 1991. A model for Neogene crustal rotations, transtension, and transpression in southern California. Geol. Soc. Am. Bull. 103, 1528–1536.
Lyons, W.B., Nezat, C.A., Carey, A.E., Hicks, D.M., 2002. Organic carbon fluxes to the ocean from high-standing islands. Geology 30, 443–446.
Madej, M.A., Ozaki, V., 1996. Channel response to sediment wave propagation and movement, Redwood Creek, California, USA. Earth Surf. Processes Landforms 21, 911–927.
Malmon, D.V., Reneau, S.L., Katzman, D., Lavine, A., Lyman, J., 2007. Suspended sediment transport in an ephemeral stream following wildfire. J. Geophys. Res. 112, F02006.
Mano, V., Némery, J., Belleudy, P., Poirel, A., 2009. Assessment of suspended sediment transport in four Alpine watersheds (France): influence of the climatic regime. Hydrol. Processes 23, 777–792.
Milliman, J.D., 1995. Sediment discharge to the ocean from small mountainous rivers: the New Guinea example. Geo-Mar. Lett. 15, 127–133.
Milliman, J.D., Farnsworth, K.L., 2011. River Discharge to the Coastal Ocean— A Global Synthesis. Cambridge University Press, Cambridge, UK, pp. 384.
Milliman, J.D., Syvitski, J.P.M., 1992. Geomorphic/tectonic control of sediment discharge to the ocean: the importance of small mountainous rivers. J. Geol. 100 (5), 525–544.
Milliman, J.D., Kao, S.-J., 2005. Hyperpycnal discharge of fluvial sediment to the ocean: impact of Super-Typhoon Herb (1996) on Taiwanese rivers. J. Geol. 113, 503–516.
Nadal-Romero, E., Regüés, D., 2010. Geomorphological dynamics of subhumid mountain badland areas—weathering, hydrological and suspended sediment transport processes: a case study in the Araguás catchment (central Pyrenees) and implications for altered hydroclimatic regimes. Progress Phys. Geogr. 34, 123–150.
Nearing, M.A., Nichols, M.H., Stone, J.J., Renard, K.G., Simanton, J.R., 2007. Sediment yields from unit-source semi-arid watersheds at Walnut Gulch. Water Resour. Res. 43, W06426.
Owens, P.N., Petticrew, E.L., van der Perk, M., 2010. Sediment response to catchment disturbances. J. Soils Sediments 10, 591–596.
Page, H.M., Reed, D.C., Brzezinski, M.A., Melack, J.M., Dugan, J.E., 2008. Assessing the importance of land and marine sources of organic matter to kelp forest food webs. Mar. Ecol. Prog. Ser. 360, 47–62.
Pinter, N., Vestal, W.D., 2005. El Nino-driven landsliding and postgrazing vegetative recovery, Santa Cruz Island, California. J. Geophys. Res. 110 (2), F02003.
Polyakov, V., Nearing, M.A., Nichols, M.H., Scott, R.L., Stone, J.J., McClaran, M., 2010. Runoff and sediment yields from small semi-arid watersheds in southern Arizona. Water Resour. Res. 46, 1–12.
Rankl, J.G., 2004. Relations between total-sediment load and peak discharge for rainstorm runoff on five ephemeral streams in Wyoming. In: USGS, Water Resources Investigations Report 02-4150. US Geological Survey, Reston Virginia.
Raphael, M., Feddema, J., Orme, A.J., Orme, A.R., 1995. The unusual storms of February 1992 in southern California. Phys. Geogr. 15, 442–464.
Rice, R.M., 1982. Sedimentation in the chaparral: how do you handle unusual events? In: Sediment Budgets and Routing in Forested Drainage Basins. Swanson F.J., Janda, R.J., Dunne, T., Swanston D.N. (Eds.). Pacific Northwest Forest and Range Experiment Station, General Technical Report PNW-141.
Rice, R.M., Foggin III, G.T., 1971. Effect of high intensity storms on soil slippage on mountainous watersheds in southern California. Water Resour. Res. 7, 1485–1496.
Roseen, R.M., Ballestero, T.P., Fowler, G.D., Guo, Q., Houle, J., 2011. Sediment monitoring bias by automatic sampling in comparison with large volume sampling for parking lot runoff. J. Irrig. Drain. Eng. 137 (4), 251–257.
Rustomji, P., Wilkinson, S., 2008. Applying bootstrap resampling to quantify uncertainty in fluvial suspended sediment loads estimated using rating curves. Water Resour. Res. 44, W09435.
Scott, K.M., Williams, R.P., 1978. Erosion and Sediment Yield in the Transverse Ranges, Southern California. U.S. Geological Survey Paper 1030, Palo Alto, CA, pp. 37 p.
Seeger, M., Errea, M.P., Beguerıa, S., Arnáez, J., Martı, C., Garcıa-Ruiz, J.M., 2004. Catchment soil moisture and rainfall characteristics as determinant factors for discharge/suspended sediment hysteretic loops in a small headwater catchment in the Spanish Pyrenees. J. Hydrol. 288 (3), 299–311.
Shakesby, R.S., Doerr, S.H., 2006. Wildfire as a hydrological and geomorphological agent. Earth-Sci. Rev. 74, 269–307, http://dx.doi.org/10.1016/j.earscirev.2005.10.006.
Syvitski, J.P., Milliman, J.D., 2007. Geology, geography, and humans battle for dominance over the delivery of fluvial sediment to the coastal ocean. J. Geol. 115 (1), 1–19.
Taylor, B.D., 1981. Sediment management for Southern California mountains, coastal plains and shoreline; Part B, Inland sediment movements by natural processes. In: Environmental Quality Laboratory Report No. 17-B. California Institute of Technology, Pasadena.
Trimble, S.W., 1981. Changes in sediment storage in the Coon Creek basin, Driftless Area, Wisconsin, 1853 to 1975. Science 214, 181–183.
Trimble, S.W., 1997. Contribution of stream channel erosion to sediment yield from an urbanizing watershed. Science 278, 1442–1444.
Tropeano, D., 1991. High flow events, sediment transport in a small streams in the "Tertiary Basin" area in piedmont (northwest Italy). Earth Surf. Processes Landforms 16, 323–339.
van Rijn, L.C., 1984. Sediment transport, Part II: suspended load transport. J. Hydraul. Eng. 110 (11), 1613–1641.

Vörösmarty, C.J., Fekete, B.M., Meybeck, M., Lammers, R.B., 2000. Global system of rivers: Its role in organizing continental landmass and defining land-to-ocean linkages. Global Biogeochem. Cycles 14, 599–621.
Walling, D.E., 1974. Suspended sediment and solute yield from a small catchment prior to urbanization. Institute of British Geographers, Special Publication, 6, p. 167–192.
Warrick, J.A., 2002. Short-term (1997–2000) and long-term (1928–2000) observations of river water and sediment discharge to the Santa Barbara Channel, California. Ph.D. Thesis. University of California, Santa Barbara, pp. 337 p.
Warrick, J.A., 2009. Chapter 6—the impacts of debris basins on sediment delivery to the Santa Barbara littoral cell, California. In: Barnard, P.L., Revell, D.L., Hoover, D., Warrick, J.A., Brocatus, J., Draut, A.E., Dartnell, P., Elias, E., Mustain, N., Hart, P.E., Ryan, H.F. (Eds.), Coastal processes study of Santa Barbara and Ventura County. U. S. Geological Survey, California, pp. 161–182, Open-File Report 2009–1029.
Warrick, J.A., 2014. Trend analyses with river sediment rating curves. Hydrol. Processes, http://dx.doi.org/10.1002/hyp.10198.
Warrick, J.A., Barnard, P.L., 2012. The offshore export of sand during exceptional discharge from California rivers. Geology 40, 787–790.
Warrick, J.A., Mertes, L.A.K., 2009. Sediment yield from the tectonically active semi-arid Western Transverse Ranges of California. Geol. Soc. Am. Bull. 121 (7/8), 1050–1070.
Warrick, J.A., Milliman, J.D., 2003. Hyperpycnal sediment discharge from semi-arid southern California rivers—implications for coastal sediment budgets. Geology 31, 781–784.
Warrick, J.A., Rubin, D.M., 2007. Suspended-sediment rating-curve response to urbanization and wildfire, Santa Ana River, California. J. Geophys. Res.—Earth Surf. 112, F02018.
Warrick, J.A., Hatten, J.A., Pasternack, G.B., Gray, A.B., Goni, M.A., Wheatcroft, R.A., 2012. The effects of wildfire on the sediment yield of a coastal California watershed. Geol. Soc. Am. Bull. 124 (7–8), 1130–1146.
Warrick, J.A., Madej, M.A., Goñi, M.A., Wheatcroft, R.A., 2013a. Trends in the suspended-sediment yields of coastal rivers of northern California, 1955-2010. J. Hydrol. 489, 108–123.
Warrick, J.A., Simms, A.R., Ritchie, A., Steel, E., Dartnell, P., Conrad, J.E., Finlayson, D.P., 2013b. Hyperpycnal plume-derived fans in the Santa Barbara Channel, California. Geophys. Res. Lett. 40 (10), 2081–2086.
Warrick, J.A., Washburn, L., Brzezinski, M.A., Siegel, D.A., 2005. Nutrient contributions to the Santa Barbara Channel, California, from the ephemeral Santa Clara River. Estuarine, Coastal Shelf Sci. 62 (4), 559–574.
Washburn, L., McPhee-Shaw, E., 2013. Coastal transport processes affecting inner-shelf ecosystems in the California current system. Oceanography 26, 34–43.
Wells Jr., W.G., 1981. Some effect of brushfires on erosion processes in coastal southern California. In: Davies, T.R.H., Pearce, A.J. (Eds.), Erosion and Sediment Transport in Pacific Rim Steeplands, January 1981, Chirst Church, New Zealand. Sponsored jointly by the Royal Society of New Zealand, New Zealand Hydrological Society, IAHS, and the National Water and Soil Conservation Authority of New Zealand. International Association of Hydrologic Sciences Publication, 132, pp. 305–342.
Willis, C.M., Griggs, G.B., 2003. Reductions in fluvial sediment discharge by coastal dams in California and implications for beach sustainability. J. Geol. 111, 167–182.
Zabaleta, A., Martínez, M., Uriarte, J.A., Antigüedad, I., 2007. Factors controlling suspended sediment yield during runoff events in small headwater catchments of the Basque Country. Catena 71 (1), 179–190.